JACS
JOURNAL OF THE AMERICAN CHEMICAL SOCIETY
Article
pubs.acs.org/JACS

Photoswitching of a Thermally Unswitchable Molecular Magnet $Cu(hfac)_2L^{i\text{-}Pr}$ Evidenced by Steady-State and Time-Resolved Electron Paramagnetic Resonance

Irina Yu. Barskaya,[†,‡] Evgeny V. Tretyakov,[†] Renad Z. Sagdeev,[†,§] Victor I. Ovcharenko,[†] Elena G. Bagryanskaya,[†,‡,∥] Kseniya Yu. Maryunina,[†,⊥] Takeji Takui,[#,∇] Kazunobu Sato,[#,∇] and Matvey V. Fedin*[,†,‡]

[†]International Tomography Center SB RAS, Institutskaya str. 3a, 630090 Novosibirsk, Russia
[‡]Novosibirsk State University, Pirogova str.2, 630090 Novosibirsk, Russia
[§]Kazan (Volga Region) Federal University, Kremlevskaya St. 18, 420008 Kazan, Russia
[∥]N.N. Vorozhtsov Novosibirsk Institute of Organic Chemistry SB RAS, Pr. Lavrentjeva 16, 630090 Novosibirsk, Russia
[⊥]Department of Chemistry, Graduate School of Science, Hiroshima University, Higashi-Hiroshima 739-8526, Japan
[#]Department of Chemistry and Molecular Materials Science, Graduate School of Science, Osaka City University, Osaka 558-8585, Japan
[∇]FIRST-Quantum Information Processing Project, JSPS, Tokyo 101-8430, Japan

Supporting Information

ABSTRACT: Most photoswitchable molecular magnets exhibit thermally induced switching, as is typical of spin crossover (SCO), valence tautomerism and SCO-like phenomena. We report a rare case of a copper-nitroxide based molecular magnet $Cu(hfac)_2L^{i\text{-}Pr}$ that does not exhibit quantitative SCO-like behavior in the temperature range of its chemical stability (2−350 K); however, it can be switched to a metastable thermally inaccessible spin state via visible/near-IR light at cryogenic temperatures. By means of photogeneration, unique information on this otherwise unobservable spin state has been obtained using steady-state Q-band (34 GHz) and time-resolved W-band (94 GHz) electron paramagnetic resonance (EPR) spectroscopy. In particular, we have found that the electronic structure and relaxation properties of the photoinduced state in $Cu(hfac)_2L^{i\text{-}Pr}$ are very similar to those in its sister compound $Cu(hfac)_2L^{n\text{-}Pr}$ that is thermally switchable and has been exhaustively characterized by many analytical methods, previously. The first observation of photoswitchable behavior in a thermally unswitchable copper-nitroxide based molecular magnet $Cu(hfac)_2L^{i\text{-}Pr}$ paves the way for photoswitching applications of this and similar compounds in the remarkably broad temperature range of 2−350 K.

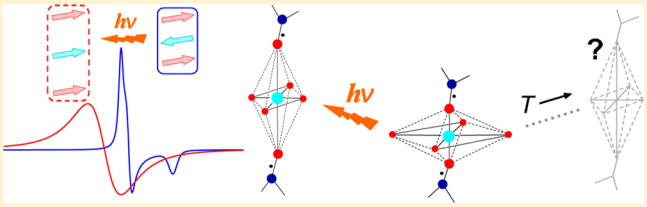

INTRODUCTION

Research on magnetoactive materials is strongly stimulated by their potential applications in spintronics, nanoscale sensing, magnetic data storage, quantum computing, etc.[1−3] In particular, spin crossover (SCO) compounds constructed from transition ions and organic ligands received great attention during the past decades.[4−9] The switching between different spin states in SCO compounds can be induced by various external stimuli including temperature, light, pressure, X-ray irradiation, etc.[10−13] Light-induced spin state switching and light-induced excited spin state trapping (LIESST) phenomena have been thoroughly investigated as promising grounds for future applications.[14−20] The photoswitching phenomena in SCO compounds combine ultrafast conversion from the ground to excited states (on the time scale of femtoseconds)[21−24] and long lifetimes of the photoinduced states at cryogenic temperatures.[4−6] The overwhelming majority of SCO compounds are based on iron(II). More recently, however, fundamentally different types of copper(II)-nitroxide based molecular magnets exhibiting SCO-like behavior have been found.[25−32] Among these, complexes $Cu(hfac)_2L^R$ (where L^R is the nitroxide ligand) may contain the two- or three-spin exchange-coupled clusters copper(II)-nitroxide or nitroxide-copper(II)-nitroxide, respectively.[29−32] We note that the SCO description in a strict manner is not applicable to complexes of copper(II), because the $3d^9$ electronic configuration excludes any possibility of different spin states. However, we emphasize that the presence of paramagnetic nitroxide ligands makes the SCO-type spin state switching possible on the scale of exchange-coupled clusters. Most of the molecular magnets $Cu(hfac)_2L^R$ known up to date

Received: May 13, 2014
Published: June 24, 2014

   dx.doi.org/10.1021/ja504774q | J. Am. Chem. Soc. 2014, 136, 10132−10138

have a polymer-chain structure with alternating spin triads of nitroxide-copper(II)-nitroxide and one-spin copper(II) units. Both thermo- and photoswitching occur in the spin triads, for which the two states involved are the weakly coupled spin (WS) state, which is characterized by weak ferromagnetic exchange between copper(II) ion and nitroxides ($|J| \ll k_BT$), and the strongly coupled spin (SS) state, where the exchange interaction is strong ($|J| \gg k_BT$) and antiferromagnetic, leading to an $S = 1/2$ ground state of the triad. Reversible thermal transitions between the WS and SS states are accompanied by unusually large changes in the volume of the unit cell (up to 13%); therefore, molecular magnets $Cu(hfac)_2L^R$ are often called "breathing crystals". Numerous compounds of this family have been studied over the past decade, and many similarities with SCO compounds have been observed. Among them, quite recently photoswitching and LIESST-like phenomena in the breathing crystals have been discovered.[33−36] The conversion from the ground SS state to the excited WS state can be induced by visible/near-IR light, and this photoinduced WS state is metastable on time scale of hours at $T < 60$ K.

Electron paramagnetic resonance (EPR) has been an indispensable tool in detecting the photoswitching in the breathing crystals: by comparison, the application of SQUID magnetometry is strongly limited due to the high optical density of the crystals (in both the SS and WS states).[33−37] The high sensitivity of EPR allows using diluted and optically more transparent samples (microcrystals in various matrices), and the application of high-frequency time-resolved (TR) EPR yields information on photoinduced spin dynamics at the nanosecond time scale.[35] In addition, very recent studies of the breathing crystals by femtosecond optical spectroscopy have evidenced that the photoswitching from the SS to WS state is an ultrafast process occurring within 50 fs.[38]

All previous studies of the photoswitching were done on the breathing crystals that (as was known beforehand) exhibit quantitatively complete thermally induced spin state switching, so that either the WS and SS states could be isolated at proper temperatures and investigated using X-ray analyses, SQUID measurements, EPR and IR spectroscopy, etc. In this paper, we report the first observation and high-frequency EPR study of a photoinduced WS state in the complex $Cu(hfac)_2L^{i\text{-}Pr}$ that cannot thermally be quantitatively generated anywhere in the temperature range of the complex's chemical stability (2−350 K). Photogeneration provides an elegant way to create this otherwise inaccessible state, and allow its characterization using Q-band steady-state and W-band TR EPR spectroscopy. We discuss the electronic structure and relaxation properties of the WS state in $Cu(hfac)_2L^{i\text{-}Pr}$, as well as new aspects of this important type of photoswitching.

EXPERIMENTAL SECTION

Synthesis, structure and magnetic properties of the polymer-chain complex $Cu(hfac)_2L^{i\text{-}Pr}$ (**I**) have been described elsewhere.[39] For comparison, in this study we also use its sister compound $Cu(hfac)_2L^{n\text{-}Pr}$ (**II**) that was previously investigated by many analytical methods in great detail.[31−35] The compounds **I** and **II** differ only by alkyl substituent (*i*-propyl vs *n*-propyl) in the nitroxide ligand, and their structures are quite similar, but their magnetic properties are noticeably different (Figure 1).

In order to optimize the conditions of sample illumination, in previous studies we used suspensions of glass-forming liquid (glycerol) with ground breathing crystals.[33−35] However, the illumination of the bulk sample still does not allow photoexcitation and photoswitching of all the microcrystals. In addition, the samples prepared in this way are not stable outside the cryocooled probe, since glycerol gradually dissolves the microcrystals. Therefore, in this work we prepared thin films of polyvinyl chloride (PVC) with the microcrystals of **I** or **II** embedded, which are perfectly stable (at least for one year) and, in addition, allow the photoswitching of nearly all clusters. A low molecular weight PVC (1 g) was dissolved in dichloroethane (200 mL). The solution was kept over solid $NaHCO_3$ at least for 24 h prior to use. The complex **I** or **II** (2 mg) was dissolved in the PVC-containing solution (0.3 mL), and then the mixture was placed into a quartz EPR tube. The tube was rotated at room temperature in a standard rotary evaporator while the pressure was reduced from 200 to 60 Torr for 1 h and then additionally kept at 60 Torr for 1 h to give brown-colored transparent films on the inner surface of the tube. After storage under ambient conditions or in a refrigerator for a few days, the obtained films gradually changed color to blue, which visually indicated formation of microcrystalline particles of $Cu(hfac)_2L^R$ embedded in the PVC matrix. In addition, the identity of compounds obtained was verified in EPR experiments (see below).

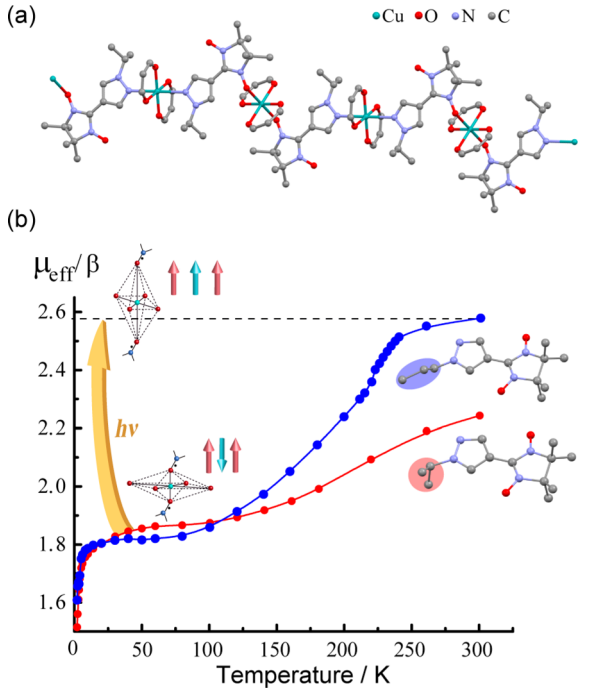

Figure 1. (a) Polymer-chain structure of the breathing crystal $Cu(hfac)_2L^{i\text{-}Pr}$ (**I**). (b) Temperature dependence of the effective magnetic moment in complexes $Cu(hfac)_2L^{i\text{-}Pr}$ (**I**, red) and $Cu(hfac)_2L^{n\text{-}Pr}$ (**II**, blue) (adapted from ref 39) with the corresponding structures of nitroxide ligands. Magnetostructural diagrams on the left illustrate the generation of the thermally inaccessible weakly coupled spin state of **I** by light at low temperatures.

Steady-state EPR measurements were carried out at Q-band (34 GHz) using a commercial Bruker Elexsys E580 EPR spectrometer. In situ illumination of **I**/**II** embedded in the PVC films was done at 900 nm using a LOTIS-TII Nd:YAG laser and OPO-system (10 Hz repetition rate, 1−2 mJ per pulse). W-band (94 GHz) time-resolved (TR) EPR experiments were carried out using a Bruker E600 spectrometer with in situ illumination at 532 nm by a Spectra Physics PRO270 Nd:YAG laser (20 Hz repetition rate, max. 0.1 mJ per pulse on the sample surface). For the W-band measurements samples must be placed in thin capillary tubes (0.5 mm I.D.); therefore, the use of frozen glycerol suspensions was technically more convenient compared to PVC films. Both the spectrometers were equipped with Oxford Instruments temperature control systems ($T = 4$−300 K). The EasySpin software toolbox was used for simulation of EPR spectra shown in Figure 2.[40]

dx.doi.org/10.1021/ja504774q | J. Am. Chem. Soc. 2014, 136, 10132−10138

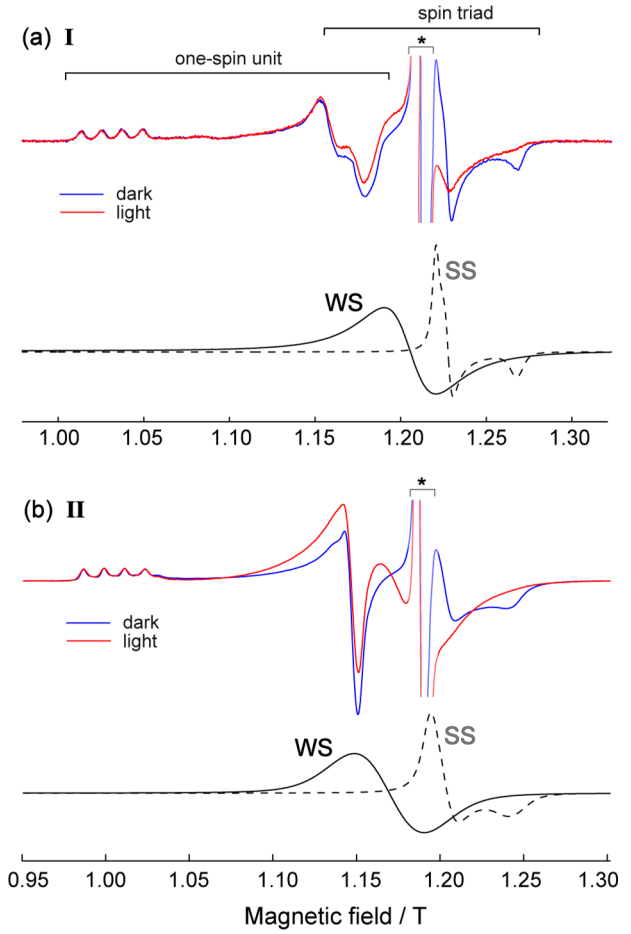

Figure 2. Q-band steady-state EPR spectra of **I** (a) and **II** (b) embedded in the PVC films recorded at 7 K before ("dark") and after ("light") 600 s illumination with 900 nm light. Spectral regions of the spin triads and one-spin copper(II) units are indicated on top. Admixtures of free nitroxide ($g \approx 2.007$) are marked with an asterisk (*). Lower panels of (a) and (b) show deconvoluted signals of the spin triads in the ground SS and photoinduced WS states (see Table 1 for parameters used).

RESULTS AND DISCUSSION

The effective magnetic moments $\mu_{eff}(T)$ of compounds **I** and **II** exhibit gradual changes over T = 4–300 K (Figure 1). For compound **II** the transition from the SS to WS state is complete, whereas the value of μ_{eff}(300 K) for compound **I** corresponds to contributions from ~56% of the WS state and ~44% of the SS state (see Supporting Information for details). In this situation, it is hardly possible to deduce reliable information on structural and magnetic properties of the WS state using XRD, SQUID magnetometry, or EPR.[41]

It is well-known for SCO compounds that their cooperative interactions depend on particle size, where downscaling the particles leads to more gradual thermal SCO.[4−6,42] One expects a similar trend for breathing crystals, and thus some differences in SCO-like behavior may be envisioned between neat polycrystalline compounds and microcrystals dispersed in PVC. Therefore, using thermoswitchable compound **II** as a reference, we first ensured that embedding microcrystals in PVC does not interfere with previously observed SCO-like phenomena. Indeed, using EPR we have found similar SCO-like behavior for **II** in PVC compared to the neat compound. As expected, a decrease of cooperativity results in a slightly more gradual thermal transition in PVC (see Supporting Information), with the conversion to the SS state upon temperature decrease being essentially finished at ~50 K (compared to 90–100 K in the neat compound).

EPR spectra of compounds **I** and **II** exhibit contributions by the spin triads and one-spin copper(II) units (Figure 2). In addition, crystallization in the PVC matrix gives admixed narrow signals of free, uncoordinated nitroxides appearing at g ~ 2.007 (~10% of the total number of spins) superimposed on the spectra of the breathing crystals. Illumination results in a dramatic change of the spin triad signals (Figure 2), which transform from intensive anisotropic signals with $g < 2$ in the dark to broad and less intense lines with $g > 2$. As has been previously studied in depth, such transformations correspond to a switch from the ground SS state to the photoinduced WS state.[33,34] The individual spectra of the SS and WS states can be readily obtained by subtraction ("light" − "dark") and simulation (see Supporting Information for details): these are plotted in the bottom panels of Figure 2a,b. The spectra of the spin triads in the low-temperature SS state are very similar for **I** and **II**, and the same holds for their photoinduced WS spin states. The characteristic parameters (g-tensors and line width) are slightly different (see Table 1), but the general similarity is obvious. Thus, Figure 2a clearly shows that the thermally inaccessible WS state of **I** can be photogenerated at cryogenic temperatures.

Table 1. EPR and Relaxation Parameters Used in the Simulations for Compounds I and II[a]

	$Cu(hfac)_2L^{i\text{-}Pr}$ (**I**)	$Cu(hfac)_2L^{n\text{-}Pr}$ (**II**)
g_{triad}(SS)	[1.990 1.977 1.919]	[1.991 1.982 1.916]
g_{triad}(WS)	2.0165	2.0336
Γ_{triad}(WS)/ mT	53.7	65.8
k_0/s^{-1}	$(3.9 \pm 0.7)\cdot10^{-2}$	$(9.8 \pm 1.7)\cdot10^{-4}$
E_A/cm^{-1}	23.3 ± 3.1	13.3 ± 5.9
σ/cm^{-1}	5 K: 11	5 K: 11
	7 K: 16	7 K: 24
	10 K: 17	10 K: 22
	13 K: 20	13 K: 27
$T_{rel}/\mu s$	5 K: 3.01	5 K: 3.32
	10 K: 2.57	10 K: 2.25
	13 K: 1.61	15 K: 1.54

[a] g_{triad} is g-tensor of the spin triad in the SS or WS state; Γ_{triad} is the EPR line width (fwhh) of the spin triad in the WS state; k_0, E_A and σ are the parameters determining the self-decelerating WS → SS relaxation (explained in the text); T_{rel} is the characteristic time of intermultiplet electron spin relaxation obtained in the TR EPR experiment.

Similarly to **II**, the photoinduced WS state of **I** is metastable at T < 20 K (Figure 3a). We have established previously that the relaxation from the metastable photoinduced WS state to the ground SS state in breathing crystals has an unusual self-decelerating character.[34] This occurs due to the broad distribution of energy barrier heights (E_A) between the WS and SS potential wells (Figure 3c). As a result, fast-relaxing centers contribute in the beginning of the relaxation curve $\gamma_n(t)$ (γ_n is the fraction of the WS state normalized to unity at t = 0), whereas slow-relaxing ones contribute to its tail, and the overall shape of the $\gamma_n(t)$ dependence appears self-decelerating. Figure 3a compares $\gamma_n(t)$ dependences vs temperature for **I** and **II**. It is evident that the relaxation in **I** is somewhat faster compared to

dx.doi.org/10.1021/ja504774q | J. Am. Chem. Soc. 2014, 136, 10132−10138

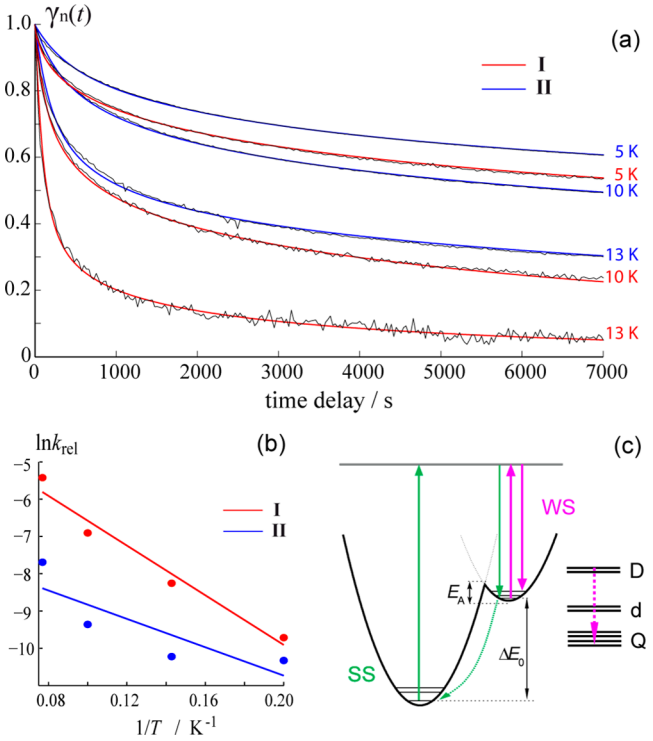

Figure 3. (a) Normalized relaxation dependence $\gamma_n(t)$ measured for **I** and **II** at T = 5−13 K (indicated on the right). Colored lines show the simulations using the parameters given in Table 1. (b) Pseudo-Arrhenius plot, ln k_{rel} vs $1/T$ for the data shown in (a) and that recorded at T = 7 K (Supporting Information). (c) Sketch of the potential energy surface for the SS and WS states. Green arrows show the SS → WS photoswitching via an intermediate excited state and structural WS → SS relaxation via quantum tunneling. Magenta arrows show the secondary excitation and relaxation process observed in the TR EPR experiments. The electronic structure of spin multiplets in case of ferromagnetic exchange coupling is shown on the right.

that in **II** at the same temperatures over T = 5−13 K. Assuming that the relaxation rate is described by a thermally activated tunneling process $k_{rel} = k_0 \cdot \exp(-E_A/k_B T)$,[34] the experimental $\gamma_n(t)$ dependences can be nicely simulated using a Gaussian distribution of the E_A value with the standard deviation parameter σ (see Table 1). In addition, Figure 3a shows that the relaxation in **I** accelerates with temperature slightly faster compared to **II**, which is clearly seen from a pseudo-Arrhenius plot $\ln(k_{rel})$ vs $(1/T)$ (Figure 3b). Thus, we find that both the E_A and k_0 values are larger for **I** compared to **II**. This conclusion is in excellent agreement with the qualitative expectation following from the Buhks theory previously applied in similar relaxation studies of SCO compounds.[5,43] The tunneling rate is faster for a larger energy difference between the SS and WS states (vertical displacement of the potential wells ΔE_0 in Figure 3c). At the same time, for larger ΔE_0, the temperature of the thermally induced spin transition is higher. Since this temperature is obviously much higher for **I** compared to **II** (Figure 1b), the faster relaxation of the photoinduced state found in **I** is fully reasonable. In addition, once again this proves the similarity between SCO in iron-based compounds and SCO-like phenomena in the breathing crystals, as well as the applicability of the developed theoretical approaches in both cases.

The E_A and k_0 values obtained for **II** in the PVC film (Table 1) are slightly different compared to those previously obtained in glycerol suspensions ($E_{A,glycerol}$= 19 ± 5 cm^{-1} and $k_{0,glycerol}$ = (3.2 ± 1.3) × 10^{-3} s^{-1}).[34] Some decrease in the k_0 value and, hence, the observed relaxation rate in the PVC film is attributable to the smaller-sized crystals on average, compared to suspensions in glycerol: the smaller and optically more transparent crystals can be photoswitched in the whole volume and become more stable toward relaxation compared to partly photoswitched bigger crystals. The latter crystals naturally experience mechanical tension on the border of two phases (and in some cases can even crack[36]), leading to faster relaxation to the ground state (this effect was previously described in ref 34).

Temperature dependence of the photoswitching amplitude ($\gamma_{max} \equiv \gamma_n(t = 0)$ vs T) represents another instructive approach to the characterization of photoswitching properties in the breathing crystals (Figure 4). Being recorded during the 10 Hz

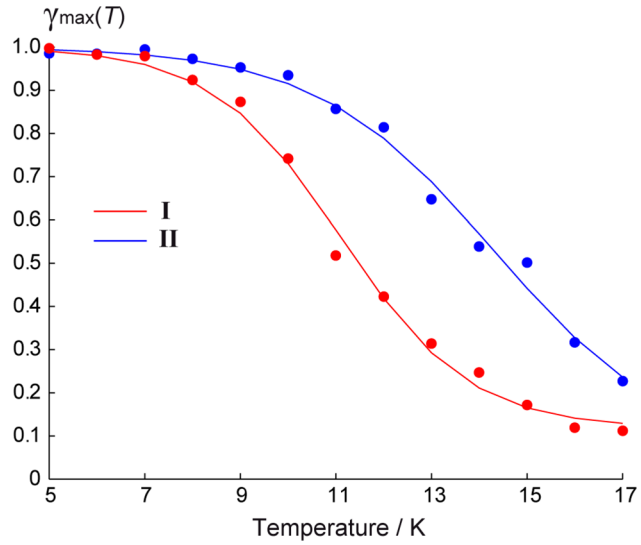

Figure 4. Maximum conversion depth $\gamma_{max} \equiv \gamma_n(t = 0)$ vs temperature for **I** and **II**. The curves are normalized to γ_{max}(5 K). Solid lines are the polynomial fits shown to "guide the eye".

laser flashing, $\gamma_{max}(T)$ corresponds to the maximum photo-induced conversion limited by a competition between the photoswitching and relaxation. In full agreement with the relaxation trends shown in Figure 3, $\gamma_{max}(T)$ dependence for **I** decays slightly faster with temperature compared to that for **II** (Figure 4), so the whole curve is shifted to lower temperatures by 3−4 K. For both compounds $\gamma_{max}(T)$ functions essentially reach their limits (plateaus) at $T \sim$ 5−7 K; thus, the photogeneration of the thermally inaccessible state of **I** is best performed at these temperatures. The net photoswitching efficiency for the sample of **II** in PVC is close to 100% (Figure 2b), while for **I** in PVC it is somewhat smaller (~67%, Figure 2a). Note that these net values are influenced by the sample morphology and instrumental setup (the percentage of the microcrystals effectively illuminated by light), whereas $\gamma_{max}(T)$ dependences are obtained after subtraction of light-independent EPR signals ("light" − "dark" spectra subtraction). Therefore, the observation of low-temperature plateaus on $\gamma_{max}(T)$ dependences is a true measure of the maximum conversion depth for the compound (not just for the particular sample or illumination conditions).

So far we have shown that (i) the thermally inaccessible WS state of **I** can be generated by light at cryogenic temperatures,

dx.doi.org/10.1021/ja504774q | J. Am. Chem. Soc. 2014, 136, 10132−10138

(ii) the WS → SS relaxation properties in **I** are generally similar to those of **II**, and (iii) the observed differences are very reasonable from theoretical considerations. The exchange coupling (the sign and the magnitude) can also be characterized in this thermally inaccessible WS state of **I**. To do this, time-resolved (TR) EPR techniques[44] have recently been found very informative for the investigation of light-induced spin dynamics in the breathing crystals.[35] The TR EPR signal at a certain magnetic field reflects the transient microwave absorption rising after the laser flash on nanoseconds to microseconds time scale, whereas all time-independent (steady-state) signals are filtered out and do not contribute. Because acquiring good TR EPR signals requires many repetitions (carried out with 20 Hz frequency in our case), and since the WS → SS relaxation in the breathing crystals takes hours at $T \sim 5-7$ K, after a few minutes of laser illumination the compound completes the transition to the WS state.[34,35] Therefore, such TR EPR experiments can operate on the WS state of the breathing crystal, and we can obtain useful information on the electronic structure of this state.

Figure 5 shows W-band TR EPR kinetics of the photo-induced WS state in **I** and **II** detected after the laser flash at T = 5−15 K (see Supporting Information for details). These kinetics are determined by an excitation/relaxation process between the spin multiplets of the WS state sketched in Figure 3c (on the right) and described in detail in ref 35. In the case of the ferromagnetic exchange coupling in the WS state, the initial drop of the kinetics at short time delays is caused by depopulation of the ground quartet state (Q), whereas the following rise is determined by electron relaxation from the excited doublet state (D) back to the ground quartet Q and can be well approximated by a monoexponential function. In case of the antiferromagnetic exchange coupling in the WS state the order of the spin multiplets shown in Figure 3c is reversed, and the expected phase of the kinetics would be the opposite. However, we observed the same phase of the TR EPR kinetics for both **I** and **II**. Since the exchange coupling in the WS state of **II** is known to be weak ferromagnetic,[31,35,45] we can safely conclude that the WS state of **I** is also characterized by a ferromagnetic coupling.

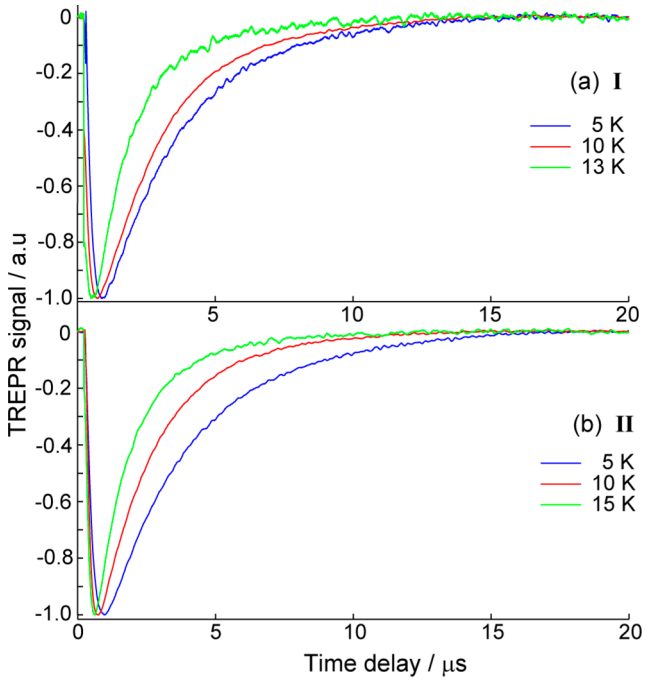

Figure 5. W-band TR EPR kinetics of the WS state of the spin triad recorded for **I** (a) and **II** (b) at T = 5−13 (15) K (indicated on the right).

The mechanism of the electron spin relaxation from the excited doublet D to the ground quartet Q of the WS state is not yet established; however, most likely it is a direct relaxation process.[35] Thus, one reasonably expects the magnitude of the intermultiplet splitting (i.e., exchange coupling) to be crucial for this relaxation rate. Figure 5 and Table 1 show that this electron spin relaxation of **I** is very close to that of **II**. Thus, not only the sign (ferromagnetic), but also the magnitude of the exchange coupling in the WS state of **I** and **II** are very similar. Previous estimates for the thermally induced WS state of **II** give the value of $|J| < 20$ cm^{-1} (for the exchange spin-Hamiltonian $H_{ex} = -2JS_1S_2$).[31,45]

At this point, we have shown that the thermally inaccessible, but photogenerated WS state of **I** has very similar electronic structure and relaxation properties compared to those of **II**. On the basis of the findings, we can reasonably speculate that the crystal structures of the WS states in both compounds are also very close, with the spin triads of **I** in the WS state framed by rhombically distorted octahedra CuO_6 with long axes along the copper-nitroxide direction (see sketch of the light-induced structure in Figure 1b; the detailed WS state structure for **II** is given in ref 39). Direct confirmation of this hypothesis by XRD is technically difficult, because the optically transparent breathing crystals have micrometer-scale sizes. Therefore, to date the high-frequency steady-state/TR EPR approaches remain methods of choice for obtaining unique information on the electronic structures and relaxation properties of the thermally inaccessible spin states in these appealing systems.

CONCLUSIONS

In this work we have shown, for the first time, the possibility of spin-state photoswitching in the unusual copper-nitroxide based molecular magnet $Cu(hfac)_2L^{i\text{-}Pr}$ that is not thermally switchable. The relevant thermally inaccessible spin state can be created using visible/near IR light at cryogenic temperatures (T < 15 K), where its long lifetime (up to several hours) allows obtaining unique information on its electronic structure and relaxation properties by steady-state and time-resolved EPR spectroscopy. Comparison with the thermally switchable compound of a very similar structure can afford further conclusions on the exchange coupling in the thermally inaccessible photoinduced state of $Cu(hfac)_2L^{i\text{-}Pr}$, as well as reasonable speculations on its geometrical structure. In this way, most important properties of the new state, relevant to further photoswitching applications, have been established.

At the same time, the possibility of photoswitching in this thermally unswitchable compound is itself the most remarkable finding. It means that one can switch the compound from the ground strongly coupled spin state to the excited weakly coupled spin state in the whole useful range of temperature, 2−350 K. Similar properties have been previously observed in only a few iron-based SCO compounds,[9,46,47] but never for copper-nitroxide based molecular magnets up to date. We note that the excited state relaxation in the breathing crystals dramatically accelerates with temperature, so that the photoinduced spin state becomes short-lived. However, our recent study using femtosecond optical spectroscopy has revealed that the

dx.doi.org/10.1021/ja504774q | J. Am. Chem. Soc. 2014, 136, 10132−10138

photoswitching in the breathing crystals is ultrafast (<50 fs),[38] and possibly even faster than in SCO compounds.[21−24] In this regard, the compound $Cu(hfac)_2L^{i\text{-}Pr}$ under study is a useful competitor for ultrafast spin-state manipulation by light, making it certainly valuable for potential applications in molecular spin devices.

■ ASSOCIATED CONTENT

Supporting Information

The estimation of the ratio between thermally switched and unswitched clusters in **I** at room temperature, the investigation of the influence of PVC matrix on thermal transition in **II**, and the details of simulation procedure for both compounds in WS and SS state. This material is available free of charge via the Internet at http://pubs.acs.org.

■ AUTHOR INFORMATION

Corresponding Author

mfedin@tomo.nsc.ru

Notes

The authors declare no competing financial interest.

■ ACKNOWLEDGMENTS

We are thankful to Dr. Hideto Matsuoka for technical help with the W-band TR EPR setup and to Professor Paul Lahti for his useful comments on our manuscript, respectively. This work was supported by RFBR (No. 14-03-00224) and RF President's Grant (MD-276.2014.3). M.V.F. thanks JSPS for granting short-term fellowship. T.T. and K.S. acknowledge Grants-in-Aid for Scientific Research on Innovative Areas "Quantum Cybernetics" and Scientific Research (B) from MEXT, Japan, and funding from the FIRST project on "Quantum Information Processing" from JSPS, Japan and from the AOARD project on "Quantum Properties of Molecular Nanomagnets" (Award No. FA2386-13-1-4030).

■ REFERENCES

(1) Leuenberger, M. N.; Loss, D. *Nature* **2001**, *410*, 789−793.
(2) Wolf, S. A.; Awschalom, D. D.; Buhrman, R. A.; Daughton, J. M.; von Molnar, S.; Roukes, M. L.; Chtchelkanova, A. Y.; Treger, D. M. *Science* **2001**, *294*, 1488−1495.
(3) Raman, K. V.; Kamerbeek, A. M.; Mukherjee, A.; Atodiresei, N.; Sen, T. K.; Lazic, P.; Caciuc, V.; Michel, R.; Stalke, D.; Mandal, S. K.; Blugel, S.; Munzenberg, M.; Moodera, J. S. *Nature* **2013**, *493*, 509−513.
(4) *Spin-Crossover Materials: Properties and Applications*; Halcrow, M. A., Ed.; John Wiley & Sons: Chichester, UK, 2013.
(5) Gütlich, P.; Goodwin, H. A. *Top. Curr. Chem.* **2004**, 233−235.
(6) Bousseksou, A.; Molnar, G.; Salmon, L.; Nicolazzi, W. *Chem. Soc. Rev.* **2011**, *40*, 3313−3335.
(7) Gaspar, A. B.; Ksenofontov, V.; Seredyuk, M.; Gutlich, P. *Coord. Chem. Rev.* **2005**, *249*, 2661−2676.
(8) Chen, J. M.; Chin, Y. Y.; Valldor, M.; Hu, Z. W.; Lee, J. M.; Haw, S. C.; Hiraoka, N.; Ishii, H.; Pao, C. W.; Tsuei, K. D.; Lee, J. F.; Lin, H. J.; Jang, L. Y.; Tanaka, A.; Chen, C. T.; Tjeng, L. H. *J. Am. Chem. Soc.* **2014**, *136*, 1514−1519.
(9) Ababei, R.; Pichon, C.; Roubeau, O.; Li, Y. G.; Brefuel, N.; Buisson, L.; Guionneau, P.; Mathoniere, C.; Clerac, R. *J. Am. Chem. Soc.* **2013**, *135*, 14840−14853.
(10) Vanko, G.; Renz, F.; Molnar, G.; Neisius, T.; Karpati, S. *Angew. Chem., Int. Ed. Engl.* **2007**, *46*, 5306−5309.
(11) Cowan, M. G.; Olguin, J.; Narayanaswamy, S.; Tallon, J. L.; Brooker, S. *J. Am. Chem. Soc.* **2012**, *134*, 2892−2894.
(12) Bousseksou, A.; Molnar, G.; Matouzenko, G. *Eur. J. Inorg. Chem.* **2004**, *22*, 4353−4369.
(13) Real, J. A.; Gaspar, A. B.; Munoz, M. C. *Dalton Trans.* **2005**, *12*, 2062−2079.
(14) Decurtins, S.; Gütlich, P.; Kohler, C. P.; Spiering, H.; Hauser, A. *Chem. Phys. Lett.* **1984**, *105*, 1−4.
(15) Gütlich, P.; Hauser, A.; Spiering, H. *Angew. Chem.* **1994**, *106*, 2109−2141; *Angew. Chem., Int. Ed. Engl.* **1994**, *33*, 2024−2054.
(16) Hauser, A. In *Topics in Current Chemistry*; Gütlich, P., Goodwin, H. A., Eds.; Springer: Heidelberg, 2004; Vol. *234*, pp 155−198.
(17) Sato, O.; Tao, J.; Zhang, Y.-Z. *Angew. Chem.* **2007**, *119*, 2200−2236; *Angew. Chem., Int. Ed.* **2007**, *46*, 2152−2187.
(18) Letard, J. F. *J. Mater. Chem.* **2006**, *16*, 2550−2559.
(19) Clemente-Leon, M.; Coronado, E.; Lopez-Jorda, M.; Waerenborgh, J. C.; Desplanches, C.; Wang, H. F.; Letard, J. F.; Hauser, A.; Tissot, A. *J. Am. Chem. Soc.* **2013**, *135*, 8655−8667.
(20) Suaud, N.; Bonnet, M. L.; Boilleau, C.; Labeguerie, P.; Guihery, N. *J. Am. Chem. Soc.* **2009**, *131*, 715−722.
(21) Cannizzo, A.; Milne, C. J.; Consani, C.; Gawelda, W.; Bressler, Ch.; van Mourik, F.; Chergui, M. *Coord. Chem. Rev.* **2010**, *254*, 2677−2686.
(22) Bertoni, R.; Lorenc, M.; Tissot, A.; Servol, M.; Boillot, M.-L.; Collet, E. *Angew. Chem.* **2012**, *124*, 7603−7607; *Angew. Chem., Int. Ed.* **2012**, *51*, 7485−7489.
(23) Bressler, C.; Milne, C.; Pham, V. T.; ElNahhas, A.; van der Veen, R. M.; Gawelda, W.; Johnson, S.; Beaud, P.; Grolimund, D.; Kaiser, M.; Borca, C. N.; Ingold, G.; Abela, R.; Chergui, M. *Science* **2009**, *323*, 489−492.
(24) Smeigh, A. L.; Creelman, M.; Mathies, R. A.; McCusker, J. K. *J. Am. Chem. Soc.* **2008**, *130*, 14105.
(25) Luneau, D.; Rey, P. *Coord. Chem. Rev.* **2005**, *249*, 2591−2611.
(26) Okazawa, A.; Hashizume, D.; Ishida, T. *J. Am. Chem. Soc.* **2010**, *132*, 11516−11524.
(27) Baskett, M.; Paduan, A.; Oliveira, N. F.; Chandrasekaran, A.; Mague, J. T.; Lahti, P. M. *Inorg. Chem.* **2011**, *50*, 5060−5074.
(28) Depanthou, F. L.; Belorizky, E.; Calemczuk, R.; Luneau, D.; Marcenat, C.; Ressouche, E.; Turek, P.; Rey, P. *J. Am. Chem. Soc.* **1995**, *117*, 11247−11253.
(29) Ovcharenko, V. I.; Bagryanskaya, E. G. In *Spin-Crossover Materials: Properties and Applications*; Halcrow, M. A., Ed.; John Wiley & Sons: Chichester, UK, 2013; pp 239−280.
(30) Ovcharenko, V. I.; Fokin, S. V.; Romanenko, G. V.; Shvedenkov, Yu. G.; Ikorskii, V. N.; Tretyakov, E. V.; Vasilevskii, S. F. *J. Struct. Chem.* **2002**, *43*, 153−167.
(31) Veber, S. L.; Fedin, M. V.; Potapov, A. I.; Maryunina, K. Yu.; Romanenko, G. V.; Sagdeev, R. Z.; Ovcharenko, V. I.; Goldfarb, D.; Bagryanskaya, E. G. *J. Am. Chem. Soc.* **2008**, *130*, 2444−2445.
(32) Fedin, M. V.; Veber, S. L.; Maryunina, K. Yu.; Romanenko, G. V.; Suturina, E. A.; Gritsan, N. P.; Sagdeev, R. Z.; Ovcharenko, V. I.; Bagryanskaya, E. G. *J. Am. Chem. Soc.* **2010**, *132*, 13886−13891.
(33) Fedin, M.; Ovcharenko, V.; Sagdeev, R.; Reijerse, E.; Lubitz, W.; Bagryanskaya, E. *Angew. Chem.* **2008**, *120*, 7003−7005; *Angew. Chem., Int. Ed.* **2008**, *47*, 6897−6899.
(34) Fedin, M. V.; Maryunina, K. Yu.; Sagdeev, R. Z.; Ovcharenko, V. I.; Bagryanskaya, E. G. *Inorg. Chem.* **2012**, *51*, 709−717.
(35) Fedin, M. V.; Bagryanskaya, E. G.; Matsuoka, H.; Yamauchi, S.; Veber, S. L.; Maryunina, K. Yu.; Tretyakov, E. V.; Ovcharenko, V. I.; Sagdeev, R. Z. *J. Am. Chem. Soc.* **2012**, *134*, 16319−16326.
(36) Drozdyuk, I. Yu.; Tolstikov, S. E.; Tretyakov, E. V.; Veber, S. L.; Ovcharenko, V. I.; Sagdeev, R. Z.; Bagryanskaya, E. G.; Fedin, M. V. *J. Phys. Chem. A* **2013**, *117*, 6483−6488.
(37) Veber, S. L.; Fedin, M. V.; Maryunina, K. Yu.; Boldyrev, K. N.; Sheglov, M. A.; Kubarev, V. V.; Shevchenko, O. A.; Vinokurov, N. A.; Kulipanov, G. N.; Sagdeev, R. Z.; Ovcharenko, V. I.; Bagryanskaya, E. G. *J. Phys. Chem. A* **2013**, *117*, 1483−1491.
(38) Kaszub, W.; Marino, A.; Lorenc, M.; Collet, E.; Bagryanskaya, E. G.; Tretyakov, E. V.; Ovcharenko, V. I.; Fedin, M. V. (submitted).
(39) Ovcharenko, V. I.; Maryunina, K. Yu.; Fokin, S. V.; Tretyakov, E. V.; Romanenko, G. V.; Ikorskii, V. N. *Russ. Chem. Bull. Int. Ed.* **2004**, *53*, 2406−2427.
(40) Stoll, S.; Schweiger, S. *J. Magn. Reson.* **2006**, *178*, 42−55.

(41) Fedin, M. V.; Veber, S. L.; Romanenko, G. V.; Ovcharenko, V. I.; Sagdeev, R. Z.; Klihm, G.; Reijerse, E.; Lubitz, W.; Bagryanskaya, E. G. *Phys. Chem. Chem. Phys.* **2009**, *11*, 6654−6663.
(42) Larionova, J.; Salmon, L.; Guari, Y.; Tokarev, A.; Molvinger, K.; Molnar, G.; Bousseksou, A. *Angew. Chem., Int. Ed.* **2008**, *47*, 8236−8240.
(43) Buhks, E.; Navon, G.; Bixon, M.; Jortner, J. *J. Am. Chem. Soc.* **1980**, *102*, 2918.
(44) Forbes, M. D. E.; Jarocha, L. E.; Sim, S.; Tarasov, V. F. *Adv. Phys. Org. Chem.* **2013**, *47*, 1−83.
(45) Veber, S. L.; Fedin, M. V.; Maryunina, K. Yu.; Potapov, A.; Goldfarb, D.; Reijerse, E.; Lubitz, W.; Sagdeev, R. Z.; Ovcharenko, V. I.; Bagryanskaya, E. G. *Inorg. Chem.* **2011**, *50*, 10204−10212.
(46) Costa, J. S.; Balde, C.; Carboner, C.; Denux, D.; Wattiaux, A.; Desplanches, C.; Ader, J.-P.; Gutlich, P.; Letard, J.-F. *Inorg. Chem.* **2007**, *46*, 4114−4119.
(47) Renz, F.; Oshio, H.; Ksenofontov, V.; Waldeck, M.; Spiering, H.; Gultich, P. *Angew. Chem., Int. Ed.* **2000**, *20*, 3699−3700.